Thermogravimetric Analysis and Pyrolysis Kinetics of Tannery Wastes in an Inert Atmosphere

by

Lan Luo,[a] Jie Liu,[a]* Cheng-Kung Liu,[b] Eleanor M. Brown,[b] Fang Wang,[a] Yadi Hu[a] and Keyong Tang[a]*
[a]*School of Materials Science and Engineering, Zhengzhou University,* Zhengzhou, Henan 450001, China
[b]*Eastern Regional Research Center, United States Department of Agriculture,*** Wyndmoor, PA 19038, USA

Abstract

Industrial wastes generated from tanneries contain large quantities of water-insoluble proteins, which may be used for the production of composite materials, renewable chemicals and energy. In this work, the pyrolysis kinetics of powdered sheep fur wastes (SFW) was studied by thermogravimetry (TG) at different heating rates from room temperature to 600°C in nitrogen atmosphere. TG results revealed that there are three stages in this process. The overall apparent activation energy (E) in the main pyrolysis stage was determined to be 275.6 kJ mol^{-1} by modified Kissinger-Akahira-Sunose (MKAS) method. Because the pyrolysis of SFW could not be described by a single-step reaction, the experimental DTG curve of SFW was deconvoluted into three individual peaks followed by reconstruction of TG curves corresponding to three pseudo components. The average values of E obtained for these pseudo components are 234.7 kJ mol^{-1}, 176.4 kJ mol^{-1}, and 186.2 kJ mol^{-1}, respectively. Generalized master-plots method indicated that the SFW pyrolysis may follow the random nucleation and growth mechanism (Avrami-Erofeev model). Reaction model functions $f(\alpha)$ for these pseudo components could be expressed as: $f(\alpha)=3.1(1-\alpha)[-\ln(1-\alpha)]^{0.67}$; $f(\alpha)=3.6(1-\alpha)[-\ln(1-\alpha)]^{0.72}$, and $f(\alpha)=3.9(1-\alpha)[-\ln(1-\alpha)]^{0.74}$, respectively. These results may provide insight for further studies as well as for future application of pyrolysis technology for tannery wastes.

Introduction

Both leather-making and fur-making have long been regarded as pollution sources to the environment, partly due to the generation of a huge amounts of solid and liquid wastes.[1-4] According to a statistical research, only about 30% of the raw hides are eventually converted into valuable leather/fur products.[1] The wastes generated in leather and fur industry may reach up to 4~6 million tons per year.[2, 4] Among them, about 150,000 and 60,000 tons of solid wastes are discharged in India and the United States of America, respectively. In China, it was estimated that around 1.4 million tons of solid waste are being generated annually.[3, 4] The disposal of tannery wastes gives rise to negative impact on the environment. Meanwhile, the costs of disposal will put a heavy burden on the industry as well as the government. Tannery waste is an important and urgent environmental issue in many countries and districts.

Except for the small quantities of leather chemicals and fats, the predominant organic components in tannery solid wastes are water-insoluble proteins (mainly collagen and keratin). With the development of economy and the improvement of human environmental awareness, it is generally accepted that there is great necessity to develop economical and environment-friendly technique for reusing these tannery solid wastes. The preferable methods of reusing leather/fur solid wastes include the preparation of composites materials or carbonaceous materials, the acquisition of energy, and the extraction of proteins or salts. Various value-added products based on recycled solid tannery wastes have been developed, such as polymer-based composite films or sheets, regenerated leather, animal feeds, fertilizers, surfactants and adhesives.[5-12]

Tannery wastes can be turned into fibers or powders via mechanical grinding process, providing a convenient way to develop composite materials from these wastes.[5] In our previous work, vegetable-tanned leather fibers were incorporated into gelatin matrices to fabricate composite films.[6] To produce polymer composites systems for various applications, examples have shown that more composites could be prepared by blending leather fibers with PVA,[7] plant fibers,[8] ABS,[9] polyurethane [10] etc. However, high temperature is always required in modern processing techniques (eg. injection molding, extrusion, calendaring, and laminating) for the phase transformation of polymer from solids to melts. Similar to other solid tannery wastes, sheep fur wastes (SFW) undergo complicated physical and chemical changes during heating process, and less is known about them.

In addition, it is possible to recycle the protein wastes from tanneries by pyrolysis technique in a more environmentally friendly manner. Banon et al. studied the pyrolysis of chrome tanned leather treated

*Corresponding authors E-mail: liujie@zzu.edu.cn; kytang@zzu.edu.cn
Manuscript received November 11, 2019, accepted for publication December 29, 2019.

**Mention of trade names or commercial products in this article is solely for the purpose of providing specific information and does not imply recommendation or endorsement by the U. S. Department of Agriculture. USDA is an equal opportunity provider and employer.

with NaOH under different conditions leading to an economic way to conserve energy and alleviate leather waste.[11] Kantarli et al. produced activated carbon materials from the shavings of chromium- and vegetable-tanned leathers.[12] Marcilla et al. developed an approach for recycling tannery wastes under fast and slow pyrolysis conditions.[13] These studies indicated that more nitrogenated compounds and phenols were produced with tanned leather compared to those with pure collagen. Yılmaz et al. investigated the production of oil, carboneous residue, ammonium carbonate and char by the pyrolysis of chromium-and vegetable-tanned shavings, as well as buffing dust.[14] Thus, it is of great importance to know the thermal behaviors and kinetics of tannery wastes before any attempts are made to reuse them.[15,16] Rosu et al. studied the influence of different tanning agents on thermal degradation behavior of leather.[17] In our previous work, we evaluated the effects of calcium carbonate on the thermal stability and decomposition kinetics of leather fiber by thermogravimetry.[18]

Sheep fur is produced by tanning the sheep skin together with dying treatment and then processing for the production of clothes, shoes, gloves, carpets, cushions and other indoor products. A large amount of sheep skin is used annually in the fur industry which generates plenty of solid waste containing protein. SFW is a very complicated material system mainly composed of collagen and keratin. Collagen is the major component in skins which might be crosslinked by tanning agents. Keratin is a strong structural protein in wool with high stability and low solubility due to the high degree of cross-linkages by disulfide and hydrogen bonds. It is not practical, in terms of time and energy, to separate the individual components of sheep fur waste. On the other hand, co-pyrolysis has received considerable attention in recent years because of the possibility for environmental-friendly transformation of biomass wastes to valuable products.[19] Therefore, pyrolysis offers a possible and convenient way to utilize such kind of solid wastes making it easy for the recovery of both energy and matter.[20-22] Besides, by knowing the thermal pyrolysis behavior and kinetics, we may take better advantage of these fibrous materials for the production of composites. To the best of our knowledge, very few studies have been conducted to examine the pyrolysis behavior of fur wastes.

In this work, sheep fur waste scraps were first ground into fiber powders and then subjected to thermogravimetric analysis in an inert atmosphere. To calculate apparent activation energy isoconversional and deconvolution methods were used. The reaction mechanism for SFW pyrolysis was studied by generalized master-plots method. The results suggested that these methods could be used in determining the kinetic model despite the complexity of the pyrolysis process.

Experimental

Materials

The sheep fur (double-face sheep leather) waste scraps in the dry state was generously provided by Prosper Skins & Leather Enterprise Co., Ltd., Henan, China, with the original appearance shown in Figure 1(a). The sheep fur was produced by chrome tanning followed by dyeing. The sheep fur waste scraps were cut into approximately 50×50 mm pieces, and then ground into powders at 8000 rpm for a total of 20 seconds using an ultra-centrifugal mill machine (ZM200, Verder Shanghai Instruments and Equipment Co., Ltd., Shanghai, China). The obtained SFW fiber powders (Figure 1(b)) were vacuum dried at 40°C for 24 h to remove excess moisture and stored at room temperature over silica gels for subsequent use.

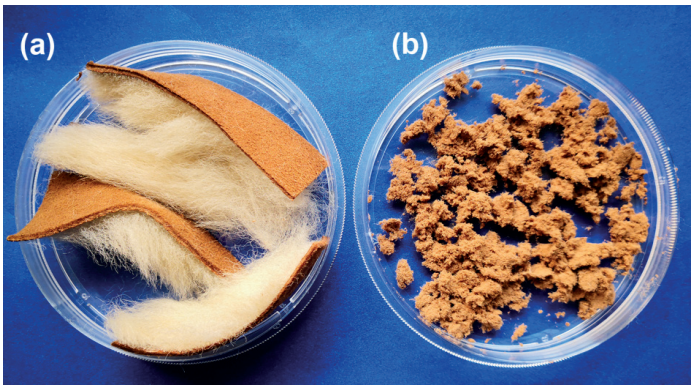

Figure 1. (a) sheep fur waste scraps and (b) ground fiber powders.

Thermogravimetric analysis (TGA)

Thermogravimetric analysis of the SFW fiber powders was carried out using a TGA/DSC1 thermogravimetric analyzer (Mettler Toledo, Switzerland). About 10 mg of fiber sample was uniformly spread on the bottom of the alumina crucible of the analyzer. The pyrolysis tests of SFW were performed at heating rates of 5, 10, 20, and 30°C min^{-1} in a dynamic nitrogen flow of 40 ml·min^{-1} from room temperature to 600°C.

Thermal analysis kinetics

Generally, thermal analysis can be studied under isothermal or non-isothermal conditions. Non-isothermal method is extremely useful for easy analysis of the thermal kinetics. Because rigorous isothermal experiments are usually difficult to be conducted, non-isothermal analysis is gradually becoming the core of thermal analysis kinetics. In describing the relationship between the reaction rate constant *k(T)* and the thermodynamic temperature T, the Arrhenius formula is often used:

$$k = Ae - \frac{E}{RT} \quad (1)$$

where E is the apparent activation energy (kJ mol^{-1}); A is the pre-exponential factor (min^{-1}); T is the thermodynamic temperature (K and R is the universal gas constant (8.314 J K^{-1} mol^{-1}). When the heating rate β is definite the kinetic equation of the heterogeneous reaction might be expressed as:

$$\beta\left(\frac{d\alpha}{dT}\right) = Af(\alpha)\exp\left(-\frac{E}{RT}\right) \quad (2)$$

where α is the conversion indicating the degree of progress in the heterogeneous system; $f(\alpha)$ is a temperature-dependent function of conversion in differential form representing the reaction model.

From the point of view of computation, the most straightforward way to achieve the objectives of kinetic analysis is the acquisition of the kinetic triplet (a set of *E*, *A* and *f*(α)). For any single-step process the simulation or prediction of the TG or DTG curves is possible when a set of triplet is obtained. For multi-step processes several kinetic triplets would be sufficient to predict the process kinetics.[23] This is important for the practical use of the knowledge of pyrolysis kinetics because it may help to predict the lifetime of the products or to design the thermochemical process reactors.

Isoconversional methods

The general idea in thermal analysis kinetics (TAK) is to use the knowledge of chemical kinetics to study the relationship between the rate of change of physical quantities measured by thermal analysis and temperature. Isoconversional methods are often used to obtain the apparent activation energy without determining any particular form of the reaction model. All isoconversional methods are based on the assumption that the reaction rate at constant α is only a function of T. There are various differential and integral forms of model-free iso-conversional analytical techniques that have been used and reported in TAK. In this study, modified Kissinger-Akahira-Sunose (MKAS) was applied to obtain the apparent activation energy for the pyrolysis of SFW.

MKAS method:[23]

$$1n\left(\frac{\beta_i}{T_{\alpha,i}^{1.92}}\right) = Cost - 1.0008\left(\frac{E_a}{RT_a}\right) \quad (3)$$

where the subscript α denotes the corresponding parameter at certain conversion.

Generalized master plots method

In order to determine the appropriate reaction model $f(\alpha)$, generalized master plots method was applied in this study.[24] In this method a parameter called generalized time (θ) was defined as:

$$\theta = \int_0^t e^{(-E/RT)}\,dt \quad (4)$$

The reduced generalized reaction rate $(d\alpha/d\theta)$ can be deduced by differentiating Eq. (4) with respect to *t*, followed by combining with Eq. (1):

$$\frac{d\alpha}{d\theta} = Af(\alpha) \quad (5)$$

Using the α=0.5 as reference point, Eq. (5) can be written as:

$$\frac{d\alpha/d\theta}{(d\theta/d\alpha)_{0.5}} = \frac{f(\alpha)}{f(0.5)} \quad (6)$$

In addition, the following equation can be derived from Eqs. (1) and (5):

$$\frac{d\alpha}{d\theta} = \frac{d\alpha}{dt}\,e^{E/RT} \quad (7)$$

Thus, Eq (6) can be expressed as:

$$\frac{d\alpha/d\theta}{(d\alpha/d\theta)_{0.5}} = \frac{d\alpha/dt}{(d\alpha/dt)_{0.5}} = \frac{e^{(E/RT)}}{e^{(E/RT_{0.5})}} \quad (8)$$

where $T_{0.5}$ denotes the temperature at the α *of* 0.5. For a single-step process the most probable kinetic model can be estimated by comparing the experimental and theoretical master plots.[24] The theoretical master plots were obtained from the commonly used kinetic model for solid-state reactions (Table I).

Table I

Commonly used kinetic models for solid-state reactions.[23]

Reaction mechanism	Symbol	f(α)	g(α)
Nucleation	An	$n(1-\alpha)[-\ln(1-\alpha)]^{(n-1)/n}$	$[-\ln(1-\alpha)]^{1/n}$
Random nucleation and nuclei growth (Avrami-Erofeev, n=2)	A2	$2(1-\alpha)[-\ln(1-\alpha)]^{1/2}$	$[-\ln(1-\alpha)]^{1/2}$
Random nucleation and nuclei growth (Avrami-Erofeev, n=3)	A3	$3(1-\alpha)[-\ln(1-\alpha)]^{2/3}$	$[-\ln(1-\alpha)]^{1/3}$
Random nucleation and nuclei growth (Avrami-Erofeev, n=4)	A4	$4(1-\alpha)[-\ln(1-\alpha)]^{3/4}$	$[-\ln(1-\alpha)]^{1/4}$
One dimensional diffusion	D1	$1/2\alpha$	α^2
Two dimensional diffusion (Valensi)	D2	$[-\ln(1-\alpha)]^{-1}$	$(1-\alpha)\ln(1-\alpha)+\alpha$
Contracting geometry	D3	$3/2(1-\alpha)^{2/3}[1-(1-\alpha)^{1/3}]^{-1}$	$[1-(1-\alpha)^{1/3}]^2$
Reaction order	Fn	$(1-\alpha)^n$	$(1/(n-1))\,[(1-\alpha)^{-(n-1)}-1]$
Contracting geometry	Rn	$n(1-\alpha)^{(n-1)/n}$	$1-(1-\alpha)^{1/n}$

After determining the kinetic model the pre-exponential factor A can be calculated by the following function:

$$g(\alpha)=\frac{AE}{\beta R}P(u) \quad (9)$$

where g(α) is the reaction function in integrated form; $u=E/RT$; $P(u)$ is the temperature integral which can be expressed by a sufficiently accurate approximation:[25]

$$P(u)=\exp(-u)/[u91.00198882u)=1.87391198] \quad (10)$$

Results and Discussion

TG/DTG curves of SFW

Figure 2 shows the weight loss and rate of weight loss (TG and DTG) curves of SFW in nitrogen atmosphere at the heating rates of 5, 10, 20 and 30°C·min^{-1}. It can be clearly found that the thermograms tend to shift to higher temperatures with increasing heating rates. These shifts are very common in all the thermogravimetric studies under non-isothermal conditions which could be explained by the presence of a temperature gradient within the sample.

In Figure 2, three stages can be distinguished from the TG curves indicating different mechanisms. The first stage appears from room temperature to 200°C, which should be related to the release of absorbed and bound water in the samples. In this region, a small hump was found in the DTG curve, centered at 74.89°C at the heating rate of 5°C min^{-1}. Proteins can absorb water by binding water molecules to their hydrophilic sites. Brebu *et al.* reported a similar peak temperature in the first weight loss stage for wool waste in inert atmosphere.[26] Leather waste also undergoes such a distinct step of water loss according to the results of other studies.[27]

In the second stage from 200 to 500°C, the major weight loss occurs, which should mainly correspond to the pyrolysis of the main components in SFW fiber powder. The pyrolysis characteristics of the sample with respect to weight loss (W_2) and the temperatures corresponding to maximum weight loss rate (T_2) for this stage, onset temperature of the main degradation (T_0), and the temperature corresponding to 50% weight loss ($T_{50\%}$) were extracted from the TG and DTG curves and listed in Table II. As is known, pyrolysis process of polymeric materials is generally affected by their composition. The shape of DTG curves implies that this stage may consist of several overlapped processes which manifested as the main and shoulder peaks (Figure 2b). This pyrolysis behavior is usually attributed to the complex thermal decomposition processes through successive and/or parallel reaction passways. In this stage, the weight loss is more than 60% of the total weight loss because of the extensive decomposition of proteinous materials. Our previous study on the thermal degradation of collagen fiber by TG-MS-FTIR and TG-FTIR revealed that both inorganic and organic fragments appear in this temperature range.[28, 29] On the other hand, the main

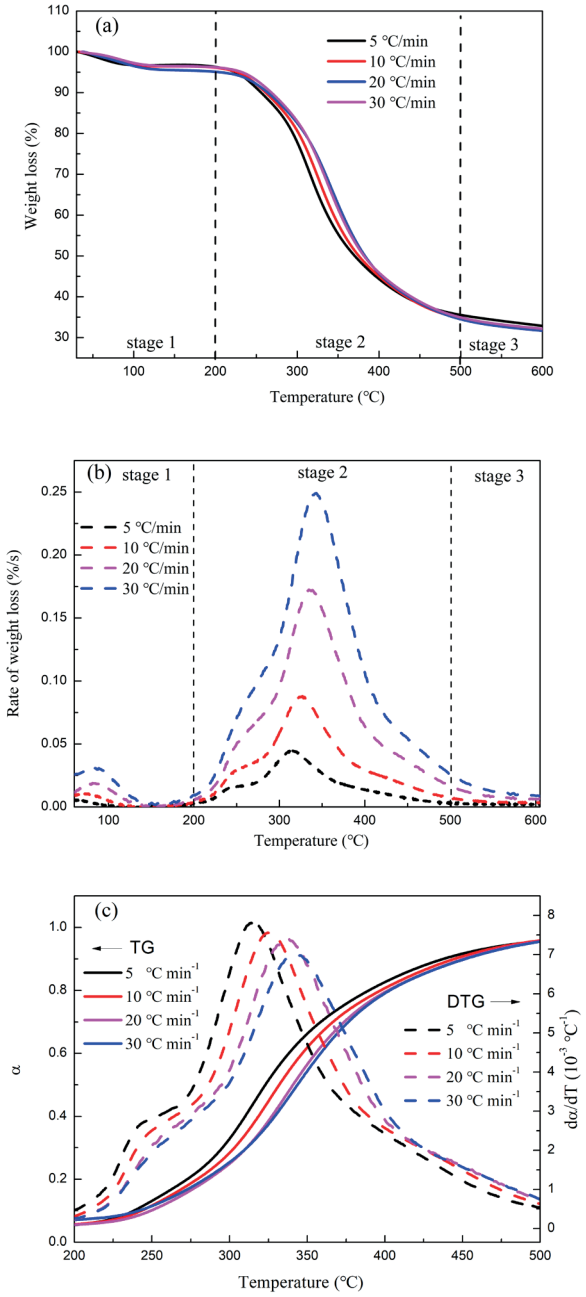

Figure 2. TG and DTG curves of sheep fur waste under various heating rates: (a) TG curves; (b) DTG curves; (c) TG and DTG profiles (from 200 to 500°C) in the forms of α vs. T (TG, solid lines) and dα/dT vs. T (DTG, dashed lines).

compounds found in the pyrolysis products of wool includes aromatics, alcohols, phenols, nitriles, etc.[30]

The last stage goes from 500 to 600°C. In this stage, the weight loss of sample was observed to occur at a significantly slower rate. It may be explained by the continuously slow decomposition of carbonaceous residues, also referred to as a second decomposition step or passive pyrolysis process at high temperatures.[31] The residue remained at 600°C (RR_{600}) are given in Table II, which decreases slightly from 32.77% to 31.55% with increasing the heating rate from 5 to 30°C min^{-1}.

Table II

Thermal degradation parameters obtained from TG and DTG curves of sheep fur waste.

β (°C min-1)	To(°C)	W2(%)	T2(°C)	T50%(°C)	RR600(%)
5	264.3	61.8	315.2	370.6	32.77
10	273.8	62.4	325.5	375.8	31.94
20	277.8	62.3	335.6	382.1	31.90
30	281.2	61.7	341.9	383.3	31.55

Note: T_0, onset temperature for stage 2; W_2, weight loss in stage 2; T_2, the temperatures corresponding to maximum weight loss rate for stage 2; $T_{50\%}$, temperature corresponding to 50% weight loss; RR_{600}, the residue remained at 600°C. W_2, $T_{50\%}$ and RR_{600} were obtained from TG curves, T_0 and T_2 were obtained from DTG curves.

TG/DTG curves of leather and wool

In order to further explore the relationship between the composition and pyrolysis behavior, the wool and leather samples obtained from the sheep fur waste scarps were ground into fiber powders separately and then subjected to thermogravimetric tests. Figure 3 shows the DTG curves (dα/dT vs. T) of the leather, wool and SFW fiber powders at the heating rate of 10°C min^{-1} in the temperature range of 200-500°C. The maximum peak temperatures of leather and wool fiber samples determined from the DTG curves are 340.3 and 335.5°C, respectively. In Figure 3, the pyrolysis of wool is complicated, and is characterized by the pronounced main peak and an evident shoulder peak at about 250°C. It has been reported that keratin contains a multi-domain peptide chain with highly retained rod-shaped intermediate regions and terminal peptide regions. Disulfide bonds are formed between keratin molecules resulting in a three-dimensional network structure which is responsible for the complex pyrolysis behavior in the DTG results.[30]

Leather sample exhibits complex pyrolysis behaviors with different characteristics too, partly attributed to the uneven crosslinking structure of the collagen network. Three overlapping peaks were observed in Figure 3. The overlapping peaks contain a main peak with two shoulders located on the right and left. Such overlaps were reported and discussed in other research works.[11, 31, 32] Bañón et al. found a shoulder in the DTG profiles of chrome tanned leather at around 450°C.[11] Xu and coworkers studied the decomposition process of wet blue of pig leather. They divided the process into three sub-reactions, relating to the pyrolysis of triglyceride, multi- and single-complexation collagen (chromium ions coordinate with collagen fibers by multi and single sites).[31] Fang et al. reported that the shoulder peak shown at 412°C of chrome-tanned leather shavings due to the overlap of lower peak and the main peak.[32]

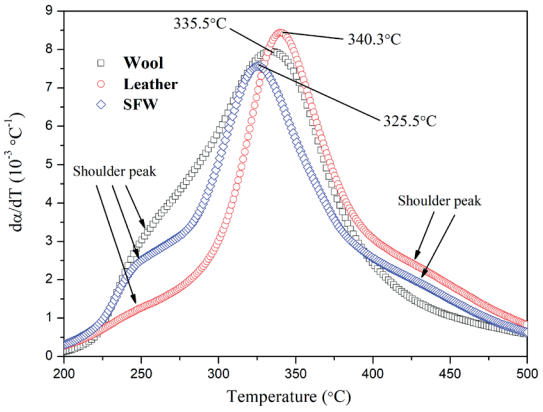

Figure 3. DTG profiles of wool, leather and SFW fiber powders in the form of dα/dT vs. Temperature.

Deconvolution method

From Figure 3, it is evident that the DTG profile of SFW is more complicated than those of leather and wool samples. The shoulder peaks at lower and higher temperatures (around 250°C and 430°C) could be attributed to the apparent sub-reactions occurring during the pyrolysis process indicating more than one mechanism in action.[33] In this case, the single-step model is not applicable to describe the reaction kinetics of the whole pyrolysis process of SFW. Using the experimental thermogravimetric data, the activation energies calculated by model-free method can only be considered as the apparent values reflecting the contributions of several sub-reactions to the overall reaction rate.

For complex processes, deconvolution method is an effective way to treat the DTG curves by separating the overlapping processes into several individual ones, followed by the application of kinetic analysis methods to these separated peaks. This approach has been frequently adopted by researchers to study the kinetics of pyrolysis by thermogravimetry.[34, 35] In the present research, initially the experimental DTG data of SFW were deconvoluted into three peaks which were assigned to three pseudo components. The use of the pseudo component concept in the pyrolysis kinetic study of SFW does not mean that each pseudo component is made up of certain

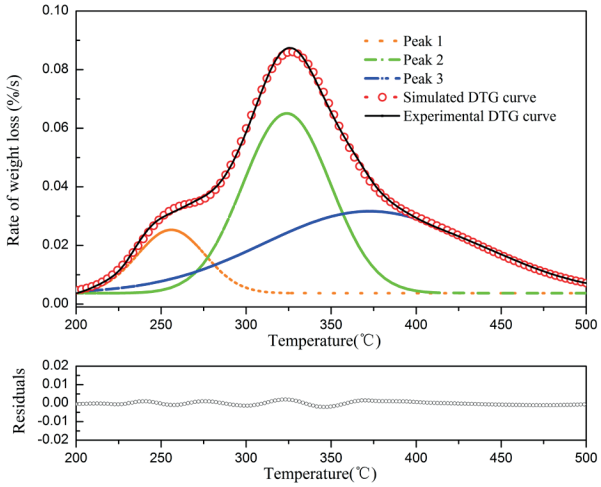

Figure 4. Experimental and deconvoluted DTG curves fitted with three Lorentz functions (heating rate: 5° min^{-1}). Residuals are shown underneath the figure.

pure, single chemical substances. In fact, it only denotes that these substances share similar pyrolysis characteristics. Herein, the pseudo components were named as PC1, PC2, and PC3 corresponding to the three deconvoluted DTG peaks (peak1, peak2, and peak 3, Figure 4) from left to right, respectively. Lorentzian distribution function is one of the most extensively used deconvolution functions. Figure 4 shows an example of the experimental and simulated DTG curves fitted with Lorentzian function. It is clear from the figure that Lorentzian function provides a good fit to the experimental DTG data. Through the deconvolution process, three sets of DTG curves corresponding to three pseudo components at different heating rates can be obtained. DTG curves are derivatives of the corresponding TG curves, while TG curves exhibit the relationship between weight loss of sample and temperature (or time). Hence, the TG curves of these pseudo components can be easily reconstructed by integrating the deconvoluted DTG profiles.

Figure 5 shows the deconvoluted DTG curves obtained from the experimental DTG data and their corresponding reconstructed TG profiles (α-T) in the temperature range of 200-500°C. These sets of the TG/DTG curves depict the weight loss behaviors of three pseudo components in the pyrolysis process. Similar trends in the TG curves towards higher temperature were observed with increasing the heating rate. At the heating rate of 10°C min^{-1}, the peak temperatures for pseudo components PC1, PC2, and PC3 are 256.7°C, 323.8°C, and 373.3°C, respectively.

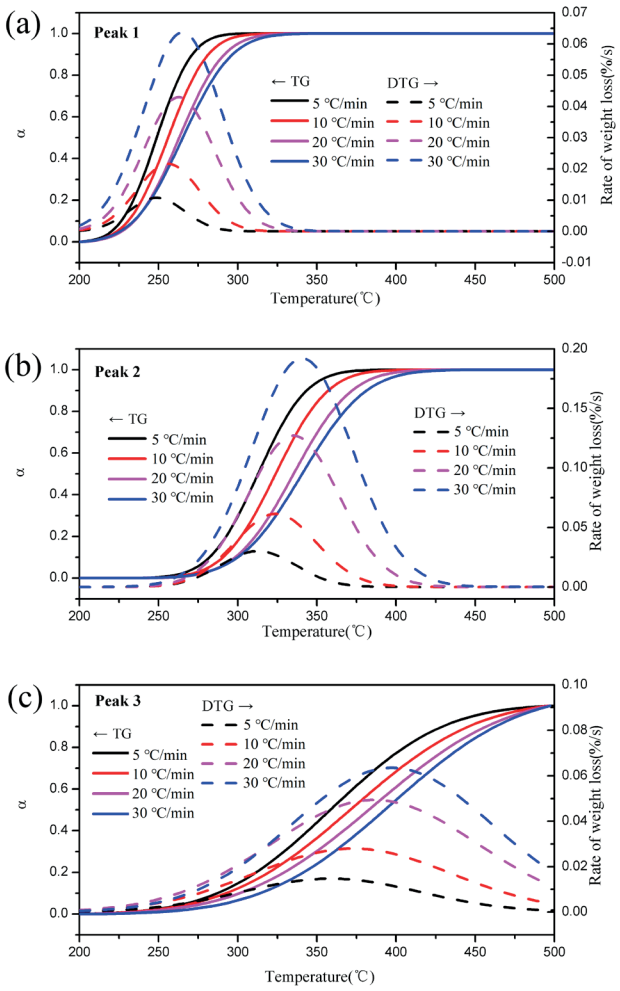

Figure 5. Deconvoluted DTG curves and their corresponding reconstructed TG profiles for the three separated peaks.

Determination of the activation energy

Model-free isoconversional methods were used to estimate the pyrolysis activation energies of SFW and its pseudo components as a function of conversion. It should be noted that isoconversional method can be applied to both single-step and multi-step processes.[23] Among the various isoconversional methods, MKAS is one of the more commonly used methods and has been considered to be more accurate than the Flynn-Wall-Ozawa method for calculating the E values.[23] According to Eq. (3), the plot of ln ($\beta/T^{1.92}$) against 1/T should be a straight line and the E value can be easily obtained from the slope at any conversion. The activation energy values of SFW and its pseudo components as obtained from the isoconversional analysis of experimental and reconstructed TG curves are shown in Figure 6. For pseudo components PC1, PC2, and PC3, the average activation energy (E_0) values are 234.7 kJ mol^{-1}, 176.4 kJ mol^{-1}, and 186.2 kJ mol^{-1}, respectively. In comparison, the E_0 value derived from the experimental TG curves of SFW is 275.6 kJ mol^{-1}. The average absolute deviations ε_E (ε_E=$|E_\alpha - E_0|\times 100/E_0$, %) are 14.7%, 6.8%, 8.6%, and 15.8% for PC1, PC2, PC3, and SFW, respectively. This result suggested that the E values calculated from the reconstructed TG curves are more consistent than those derived from experimental TG data over the conversion range 0.2-0.8. However, it can be seen from the figure that, though the deconvolution procedure was applied to the analysis of the TG results of SFW, the E value of PC1 still increases obviously with conversion level, and the ε_E of PC1 is apparently higher than those of PC2 and PC3. This is a typical feature of complex processes with different reaction mechanisms, which may be explained by the synergistic effects between the wool and leather.

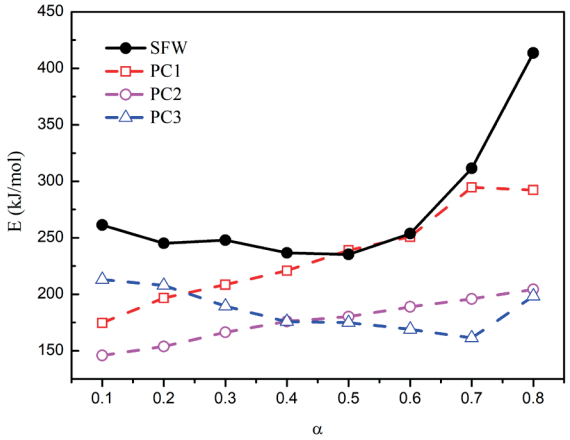

Figure 6. Activation energy values of SFW and its pseudo components as a function of conversion (α).

Master-plots Analysis

Using the temperature and dα/dt from experimental TG/DTG curves, as well as the E values determined above, $d\alpha/d\theta$ can be calculated according to Eq. (8). Accordingly, the experimental master plots of $(d\alpha/d\theta)/(d\alpha/d\theta)_{0.5}$ against α can be obtained. In the same coordinate system, a series of theoretical master plots of $f(\alpha)/f(0.5)$ against α provide reference curves, which describe the most frequently used kinetic models.[24] By comparing the experimental and theoretical master plots the most appropriate reaction functions can be roughly determined. Figure 7 shows the theoretical and experimental generalized master plots of the pyrolysis of SFW and its pseudo components. It can be seen from the figure that no existing theoretical master plots match the overall experimental master plots perfectly (Figure 7(a)). For pseudo components, the comparison of the experimental and theoretical master plots indicated that the Avrami-Erofeev equation (An model), $g(\alpha)=[-\ln(1-\alpha)]^{1/n}$, is the best to describe the kinetic process for pyrolysis of all the pseudo components (Figure 7(b)-(d)). This suggests that the reaction mechanism for these pseudo components follows the random nucleation and growth process. Besides, the experimental master plots of each pseudo component are in the same shape, no matter what heating rates were employed. Therefore, it can be concluded that the pyrolysis kinetics are independent of the heating profile and these processes can be described by single kinetic models.[23,33]

In order to further determine the optimal exponent n in A_n model, n was increased in a stepwise manner from 3.0 to 4.0 at 0.1 increments and linear least-square regression was utilized to fit the plot of $[-\ln(1-\alpha)]^{1/n}$ against EP(u)/βR according to Eq. (9). The most appropriate value of n can be determined by finding the lowest intercept (closest to 0) and highest correlation coefficient. The value of pre-exponential factor A can be derived from the slope of the plot. The kinetic triplets of all the pseudo components are listed in Table III. From pseudo component PC1 to PC3, the value of A decreases gradually, while the exponent n increases from 3.1 to 3.9 (Table III). This may be due to the variations in the composition and condition during the pyrolysis process of SFW. Based on the An model and the optimal exponent obtained above the mechanism function of PC1, PC2 and PC3 can be represented as $f(\alpha)=3.1(1-\alpha)[-\ln(1-\alpha)]^{0.67}$, $f(\alpha)=3.6(1-\alpha)[-\ln(1-\alpha)]^{0.72}$ and $f(\alpha)=3.9(1-\alpha)[-\ln(1-\alpha)]^{0.74}$, respectively.

Table III

Kinetic parameters of pyrolysis for different pseudo components of sheep fur wastes.

Pseudo components code	E (KJ mol-1)	A (min-1)	n
PC1	234.7	1.21E+22	3.1
PC2	176.4	1.64E+15	3.6
PC3	186.2	4.80E+13	3.9

The value-added utilization and pyrolysis treatment are promising approaches to reclaim energy and materials from tannery solid wastes. In order to control the pyrolysis process, the determination of pyrolysis model is necessary before the design of pyrolysis reactor,

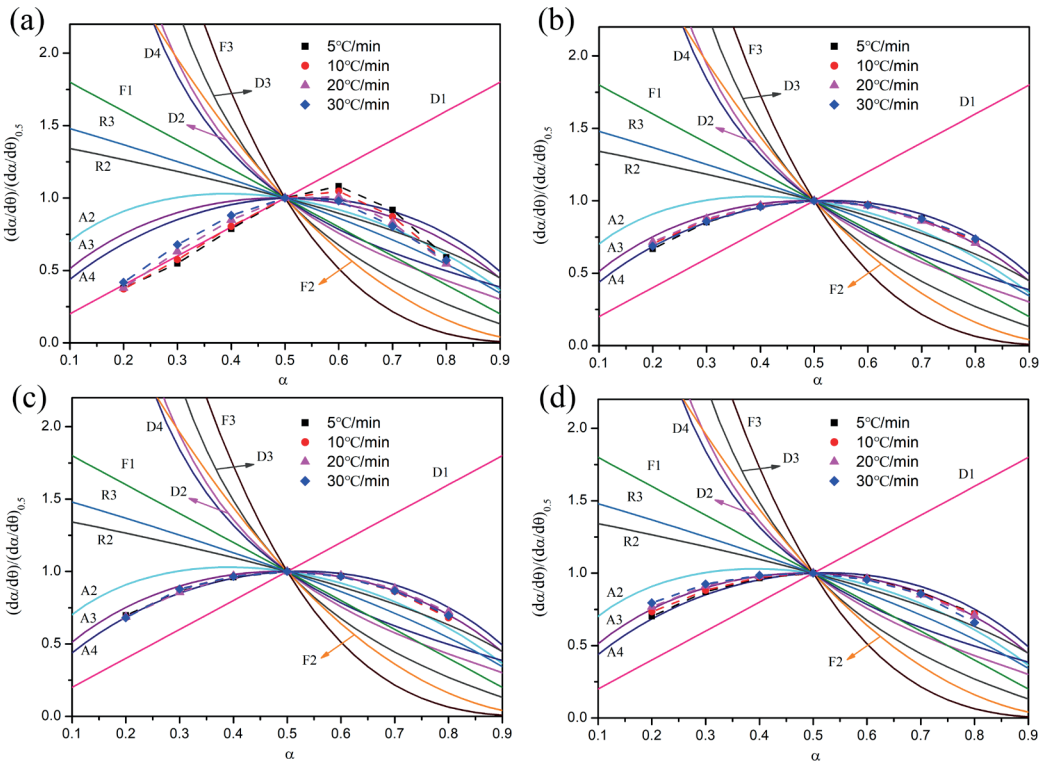

Figure 7. Theoretical and experimental master plots obtained using generalized master plots method for (a) SFW, (b) PC1, (c) PC2, and (d) PC3 pseudo components.

selection of pyrolysis conditions, and optimization of the preparation of composite materials based on tannery wastes. In the present work, the pyrolysis model for SFW was successfully established based on thermogravimetry and master plots method. Here are two examples of potential applications of the model: (1) It is difficult to perform thermogravimetric tests when the heating rates are very low and very high, this model will help to portrait the weight loss patterns and to design the pyrolysis reactor for SFW; (2) When the SFW fiber powders were used to produce composite materials, the weight loss behaviors under different heat processing conditions can be predicted with the kinetic model and parameters, which will help scientists and technicians to prevent the excessive degradation and deterioration of the bio-based fiber during the production process.

Conclusions

Three stages were distinguished for SFW during the thermogravimetric measurements in inert atmosphere. The main stage of weight loss is the second stage which corresponds to the main pyrolysis process. The pyrolysis characteristics and kinetics of SFW could not be described via a single-step reaction mainly due to complex composition and the accompanying heterogeneous features of the pyrolysis process. The experimental DTG curves of SFW were then deconvoluted into three peaks which were assigned to three pseudo components. According to the generalized master-plots method, the most probable reaction mechanism function $f(\alpha)$ for these pseudo components was: $f(\alpha)=3.1(1-\alpha)[-\ln(1-\alpha)]^{0.67}$; $f(\alpha)=3.6(1-\alpha)[-\ln(1-\alpha)]^{0.72}$ and $f(\alpha)=3.9(1-\alpha)[-\ln(1-\alpha)]^{0.74}$, respectively. These results provide insight for further studies as well as for future application of pyrolysis technology for tannery wastes.

Acknowledgements

The financial supports from the National Key Research and Development Program (2017YFB0308500), the National Natural Science Foundation Commission of China (51673177, U1204504), and Science and Technology Project of Henan Province (172102410022) are greatly appreciated.

References

1. Masilamani, D., Madhan, B., Shanmugam, G., Palanivel, S. and Narayan, B.; Extraction of collagen from raw trimming wastes of tannery: a waste to wealth approach. *Journal of Cleaner Production* **113**, 338-344, 2016.
2. Kennedy, L. J., Ratnaji, T., Konikkara, N. and Vijaya, J. J.; Value added porous carbon from leather wastes as potential supercapacitor electrode using neutral electrolyte. *Journal of Cleaner Production* **197**, 930-936, 2018.
3. Zhang, Z., Li, G. and Shi, B.; Physicochemical properties of collagen, gelatin and collagen hydrolysate derived from bovine limed split wastes. *J. Soc. Leather. Technol. Chem.* **90**, 23-28, 2006.
4. Li, Y., Guo, R., Lu, W. and Zhu, D.; Research progress on resource utilization of leather solid waste. *Journal of Leather Science and Engineering.* **1**, 6, 2019.
5. Mukhopadhyay, S. N., Saha, N., Saha, L., Saha, P. and Kolomaznik, K.; Retrieval of biodegradable polymer and value added products from leather industry waste through process biotechnology: A progress review. *JALCA* **99**, 449-456, 2004.
6. Liu, J., Liu, C-K. and Brown, E.; Development and Characterization of genipin cross-linked gelatin based composites incorporated with vegetable-tanned collagen fiber (VCF). *JALCA* **112**, 410-419, 2017.
7. Liu, Y., Wang, Q. and Li, L.; Reuse of leather shavings as a reinforcing filler for poly (vinyl alcohol). *Journal of Thermoplastic Composite Materials* **29**(3), 327-343, 2014.
8. Senthil, R., Hemalatha T., Kumar, B. S., Uma, T. S., Das, B. N. and Sastry, T. P.; Recycling of finished leather wastes: a novel approach. *Clean Technologies and Environmental Policy* **17**, 187-197, 2015.
9. Ramaraj, B.; Mechanical and thermal properties of ABS and leather waste composites. *J. Appl. Polym. Sci.* **101**, 3062-3066, 2006.
10. Członka, S., Bertino, M. F., Strzelec, K., Strąkowska, A. and Masłowski, M.; Rigid polyurethane foams reinforced with solid waste generated in leather industry. *Polymer Testing* **69**, 225-237, 2018.
11. Bañón, E., Marcilla, A., García, A., Martínez, P. and León, M.; Kinetic model of the thermal pyrolysis of chrome tanned leather treated with NaOH under different conditions using thermogravimetric analysis. *Waste Management* **48**, 285-299, 2016.
12. Kantarli, I. C., Yanik, J.; Activated carbon from leather shaving wastes and its application in removal of toxic materials. *Journal of Hazardous Materials* **179**(1-3), 348-356, 2010.
13. Marcilla, A., León, M., García, Á. N., Bañón, E. and Martínez, P.; Upgrading of tannery wastes under fast and slow pyrolysis conditions. *Ind. Eng. Chem. Res.* **51**(8), 3246-3255, 2012.
14. Yılmaz, O., Kantarli, I. C., Yuksel, M., Saglam, M. and Yanik, J.; Conversion of leather wastes to useful products. *Resources, Conservation and Recycling* **49**(4), 436-448, 2007.
15. Kluska, J., Turzyński, T. and Kardaś, D.; Experimental tests of co-combustion of pelletized leather tannery wastes and hardwood pellets. *Waste Management* **79**, 22-29, 2018.
16. Rabe, S., Sanchez-Olivares, G., Pérez-Chávez, R. and Schartel, B.; Natural Keratin and Coconut Fibres from Industrial Wastes in Flame Retarded Thermoplastic Starch Biocomposites. *Materials* **12**(3), 344, 2019.
17. Rosu, L., Varganici, C-D., Crudu, A-M. and Rosu, D.; Influence of different tanning agents on bovine leather thermal degradation. *J. Therm. Anal. Cal.* **134**, 583-594, 2008.
18. Liu, J., Brown, E.M., Uknalis, J., Liu, C-K., Luo, L. and Tang, K-Y.; Thermal stability and degradation kinetics of vegetable-tanned collagen fiber with in-situ precipitated calcium carbonate. *JALCA* **113**, 358-370, 2018.

19. Chen, C. and Wu, H.; Thermogravimetric kinetics of Chlorella pyrenoidosa and textile dyeing sludge blends during co-pyrolysis. *Energy Sources, Part A* **39**, 1469-1477, 2017.
20. Zoccola, M., Aluigi, A. and Tonin, C.; Characterisation of keratin biomass from butchery and wool industry wastes. *Journal of Molecular Structure* **938**(1-3), 35-40, 2009.
21. Senoz, E., Stanzione III, J. F., Reno, K. H., Wool, R. P. and Miller, M. E. N.; Pyrolyzed chicken feather fibers for biobased composite reinforcement. *J. Appl. Polym. Sci.* **128**, 983-989, 2013.
22. Filho, A. T., Lange, L. C., de Melo, G. C. B. and Praes, G. E.; Pyrolysis of chromium rich tanning industrial wastes and utilization of carbonized wastes in metallurgical process. *Waste Management* **48**, 448-456, 2016.
23. Vyazovkin, S., Burnham, A. K., Criado, J. M., Pérez-Maqueda, L. A., Popescu. C., and Sbirrazzuoli, N.; ICTAC Kinetics Committee recommendations for performing kinetic computations on thermal analysis data. *Thermochim. Acta* **520**, 1-19, 2011.
24. Criado, J. M., Pérez-Maqueda, L. A, Gotor, F. J., Málek, J. and Koga, N.; A unified theory for the kinetic analysis of solid state reactions under any thermal pathway. *J. Therm. Anal. Cal.* **72**, 901-906, 2003.
25. Wanjun, T., Yuwen, L., Hen, Z., Zhiyong, W. and Cunxin, W.; New temperature integral approximate formula for nonisothermal kinetic analysis. *J. Therm. Anal. Cal.* **74**, 309-315, 2003.
26. Brebu, M. and Spiridon, I.; Thermal degradation of keratin waste. *Journal of Analytical and Applied Pyrolysis* **91**, 288-295, 2011.
27. Budrugeac, P., Miu, L., Bocu, V., Wortman, F. J. and Popescu, C.; Thermal degradation of collagen-based materials that are supports of cultural and historical objects. *J. Therm. Anal. Cal.* **72**(3), 1057-1064, 2003.
28. Yang, P., He, X., Zhang, W., Qiao, Y., Wang, F. and Tang, K-Y.; Study on thermal degradation of cattlehide collagen fibers by simultaneous TG-MS-FTIR. *J Therm Anal Calorim*. **127**(3), 2005-2012, 2017.
29. Liu, J., Luo, L., Hu, Y., Wang, F., Zheng, X. and Tang, K-Y.; Kinetics and mechanism of thermal degradation of vegetable-tanned leather fiber. *Journal of Leather Science and Engineering* **1**, 9, 2019.
30. Călin, M., Constantinescu-Aruxandei, D., Alexandrescu, E., Răut, I., Doni, M. B., Arsene, M-L., Oancea, F., Jecu, L. and Lazăr, V.; Degradation of keratin substrates by keratinolytic fungi. *Electronic Journal of Biotechnology* **28**, 101-112, 2017.
31. Xu, W., Li, J., Liu, F., Jiang, Y., Li, Z. and Li, L.; Study on the thermal decomposition kinetics and flammability performance of a flame-retardant leather. *J. Therm. Anal. Cal.* **128**, 1107-1116, 2017.
32. Fang, C., Jiang, X., Lv, G., Yan, J. and Deng, X.; Nitrogen-containing gaseous products of chrome-tanned leather shavings during pyrolysis and combustion. *Waste Management* **78**, 553-558, 2018.
33. Chrissafis, K.; Kinetics of thermal degradation of polymers. *J. Therm. Anal. Cal.* **95**, 273-283, 2009.
34. Aboyade, A. O., Hugo, T. J., Carrier, M., Meyer, E. L., Stahl, R., Knoetze, J. H. and Görgens, J. F.; Non-isothermal kinetic analysis of the devolatilization of corn cobs and sugar cane bagasse in an inert atmosphere. *Thermochimica Acta* **517**(1-2), 81-89, 2011.
35. Chen, C., Miao, W., Zhou, C. and Wu, H.; Thermogravimetric pyrolysis kinetics of bamboo waste via Asymmetric Double Sigmoidal (Asym2sig) function deconvolution. *Bioresource Technology* **225**, 48-57, 2017.